Embankments on soft ground: an overview

S.V. Abhishek
Postgraduate Student, Department of Civil Engineering, A.U. College of Engineering (A), Visakhapatnam, India, <svabhi.92@gmail.com>

Madhira R. Madhav
Professor Emeritus, JNT University & Visiting Professor, IIT, Hyderabad, India <madhavmr@gmail.com>

ABSTRACT: Thick deposits of soft ground such as soft marine and estuarine clay are widespread throughout the world especially along deltas and coastal regions. Such soils possess poor geotechnical properties such as high natural moisture content (close to liquid limit), high compressibility & low shear strength. Embankments on such soft ground commonly adopted for the construction of highways, railways and airport runways are often affected by edge stability and long term settlement. The earliest method or technique employed for stable construction of embankments on soft ground was the use of vertical drains combined with stage construction. However, with growing demand for rapid construction and associated difficulty in meeting the project deadline, column-supported embankments have emerged as an appropriate technical solution. In addition, geosynthetics in the form of basal reinforcement are extensively being used at present for embankments on soft ground, to improve the bearing capacity, reduce differential settlement and prevent slope instability. A broad over-view of embankments on soft ground is presented in the present paper. The review is complemented by six well documented case histories of embankments constructed over soft ground using different geotechnical techniques. The case histories presented could help the geotechnical community to understand and evaluate the benefits of the techniques for their adoption for the construction of embankments over soft ground.

Keywords: Embankments, soft ground, pre-fabricated vertical drains, stone columns, deep cement mixed piles, basal reinforcement, soil arching

1 Introduction

Embankments form the heart of the land component of the transportation sector and are necessary to bring the elevations of existing low-lying areas up to functional elevations for roadways and railways. The construction of embankments over soft, compressible ground is increasing due to lack of suitable land for infrastructure and other developments. When constructing an embankment over very soft subsoil of low shear strength and high compressibility, the engineering tasks are to ensure stability of the embankment against possible slope failure and to control the subsoil deformation or settlement to within allowable limits.

Several methods such as stage construction with vertical drains, use of columns (such as concrete piles, stone columns and deep soil mixed piles) extending into the soft ground, and geosynthetic basal reinforcement (in the form of geotextiles, geogrids and geocells) etc, have been developed for economically and safely constructing embankments on soft ground. With such a vast variety of techniques, eventually the final choice depends upon the subsoil characteristics, project cost and time of completion, as well as the long term benefits.

This paper presents a review of embankments on soft ground. The review briefly addresses the existing methods of stability analysis for unreinforced & basal reinforced embankments, piled & basal reinforced piled embankments, embankment founded on stone columns and deep soil mixed piled embankment, over soft ground. In addition, six well documented case histories of (i) embankment on pre-fabricated vertical drain (PVD) im-

proved ground, (ii) basal reinforced embankment, (iii) piled embankment, (iv) basal reinforced piled embankment, (v) embankment on stone column treated ground and (vi) embankment on deep cement mixed piles are presented to illustrate the various technologies that can be adopted for stable construction of embankments over soft ground.

2 Stability Analysis

2.1 Unreinforced Embankment

The stability of unreinforced embankments raised on soft ground is commonly assessed using limit equilibrium analysis, wherein, different potential failure surfaces, circular and non-circular, are considered (Fig. 1).

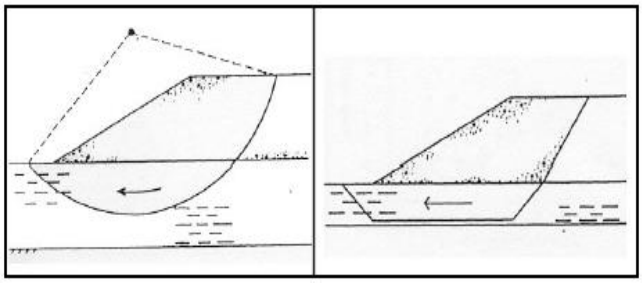

Figure 1. Circular & non-circular slip surfaces

2.2 Basal Reinforced Embankment

Embankments on soft ground are often reinforced with geosynthetics in the form of geotextiles, geogrids and geocell mattress, provided at the base (Fig. 2) to increase the factor of safety against failure (Rowe and Li 2005). The basal reinforcement increases the stability of the embankment by mobilizing tensile force in the reinforcement and also provides confinement to the embankment fill and foundation soil adjacent to the reinforcement.

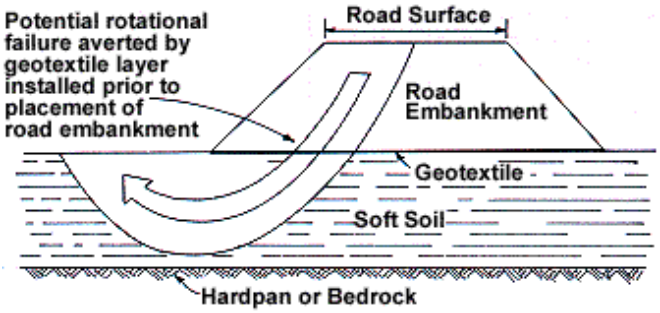

Figure 2. Basal reinforced embankment over soft soil

A number of methods are available for analysis of stability of reinforced embankments over soft ground. Some of these methods employ circular or non-circular surfaces (Milligan and Busbridge 1983; Leshchinsky 1987; Low *et al.* 1990; Kaniraj 1994), analytical solutions or plasticity theory (Davis and Booker 1973; John 1987; Houlsby and Jewell 1988; Jewell 1996), or limit equilibrium methods (Long *et al.* 1996; Bergado *et al.* 2002; Shukla and Kumar 2008).

For the purpose of embankment design, geotechnical engineers are often required to rely on either experience or on methods of analysis such as finite element methods to estimate the reinforcement strains for use in limit equilibrium calculations (Bonaparte and Christopher 1987). Use of the ultimate tensile strain of the geosynthetic reinforcement in design calculations leads to overestimation of the factor of safety since reinforced embankments may fail due to excessive displacements before failure of the reinforcement (Rowe and Soderman 1987; Rowe *et al.* 1995). To overcome the above difficulties, Rowe and Soderman (1985) introduced a method for the estimating the reinforcement strain at failure for use with slip circle analysis, but is limited to embankments constructed on soils with an approximately uniform variation of undrained shear strength with depth. However, few guidelines exist for estimating the allowable strains at failure for embankments founded on soft ground where the undrained shear strength increases with depth (Rowe and Mylleville, 1989).

2.3 Piled Embankment

Piled embankments have several advantages, viz., quick construction, small vertical and lateral deformations and improved global stability. The piles extend into and through the soft ground as shown in Fig. 3. The portions of the embankment fill between the piles have a tendency to move downward due to the high compressibility of soft foundation soil.

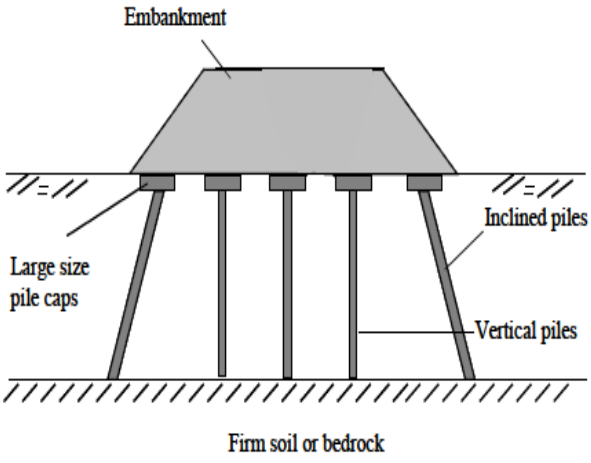

Figure 3. Piled embankment with batter piles

The movement of the embankment fill is restrained by the shear resistance mobilized in the fill, which in turn reduces the pressure on the foundation soil but increases the pressure on the pile caps. This load transfer mechanism was termed 'soil arching' by Terzaghi (1943) and is commonly evaluated by an index known as the soil arching ratio, defined as the ratio of the vertical stress above the foundation soil between the supports to the overburden stress plus surcharge, if any.

Terzaghi (1943) proposed a theoretical model assuming plane strain condition with rigid supports to describe the soil arching phenomenon after performing a series of trapdoor tests and also provided an equation to calculate the vertical stress above a yielding trapdoor (Fig. 4).

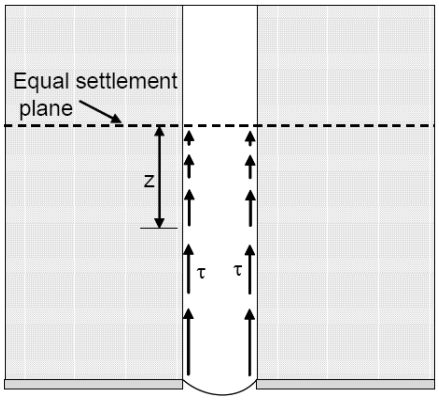

Figure 4. Soil arching model (after Terzaghi 1943)

Hewlett and Randolph (1988) derived theoretical solutions based on observations from experimental tests of actual arching in a granular soil (rather than the vertical boundaries considered by Terzaghi) for plane strain situation as shown in Fig. 5. The 'arches of sand' transmit the majority of the embankment load onto the pile caps, while the soft subsoil carries the load predominantly from the 'infill' material below the arches. The arches are assumed to be semi-circular (in two-dimensional form) and of uniform thickness with no overlap.

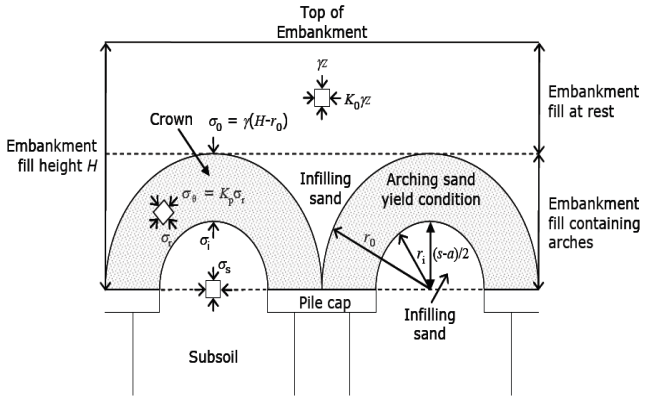

Figure 5. Soil arching above continuous supports (after Hewlett and Randolph 1988)

Hewlett and Randolph (1988) observed that soil arches forming above the piles in a square pattern possess the shape of a dome as shown in Fig. 6 and developed equivalent three-dimensional solutions for the same.

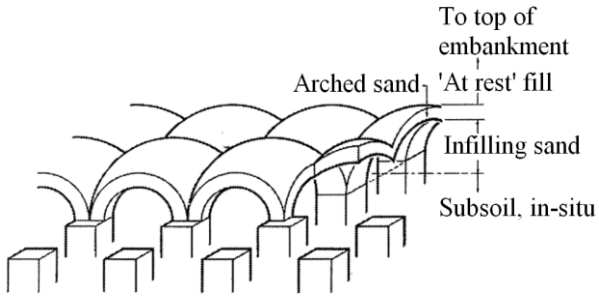

Figure 6. Soil arches above pile grid of square pattern (after Hewlett and Randolph 1988)

2.4 Basal Reinforced Piled Embankment

A basal reinforced piled embankment (Fig. 7) consists of either a single or multiple layers of geosynthetic reinforcement provided at the base.

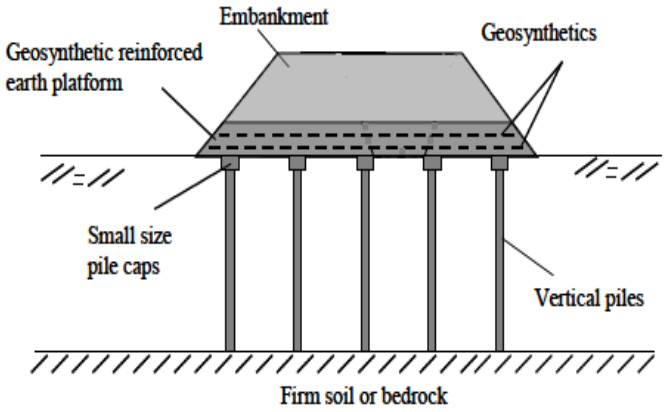

Figure 7. Basal reinforced piled embankment

A single high-strength geosynthetic layer functions as a tension membrane while a multi-layer system behaves like a stiffened platform (like a semi-rigid plate) due to the interlocking of geosynthetic reinforcement with the surrounding soil. The geosynthetic reinforcement carries the lateral thrust from the embankment, creates a stiffened platform to enhance the load transfer from the soil to the piles, and reduces differential settlement between the pile caps. The load transfer mechanism in a basal reinforced piled embankment is shown in Fig. 8. The external load and the weight of the embankment above the soil arch, are transferred to the piles via the soil arching mechanism. The embankment load below the soil arch is borne by the geosynthetic reinforcement and is transferred to the piles via geosynthetic tension. The piles then transfer the load to deeper and stiffer soil stratum.

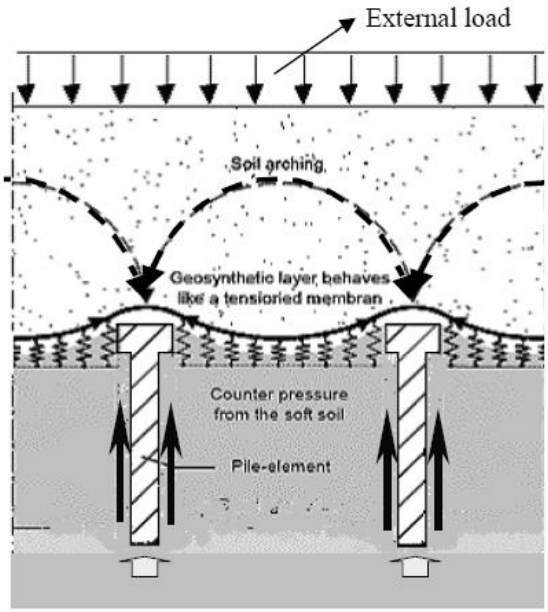

Figure 8. Load transfer mechanism in basal reinforced piled embankment

The tension in the geosynthetic reinforcement can be computed based on the tension membrane theories, the most commonly used ones being of Delmas (1979) and Giroud *et al.* (1990). Delmas (1979) developed an analytical method considering plane strain condition, to estimate the tensile deformation developed in a horizontal sheet above a trench subjected to a uniformly distributed vertical load assuming that the deformed sheet has a parabolic shape and the load remains vertical. Giroud *et al.* (1990) formulated an analytical solution to compute the tension developed in a geosynthetic sheet over a trench by assuming that the deformed sheet has a circular shape and the action of the load is normal to the deformed sheet.

2.5 Embankment Founded on Stone Columns

The stability analysis of embankments supported on stone columns involves a failure mechanism consisting of a sliding failure surface that mobilizes shear strength of the soil and the columns.

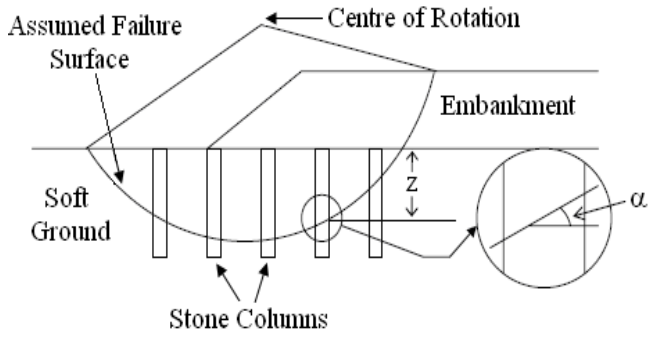

Figure 9. Circular sliding surface method for stone columns (after Aboshi *et al.* 1979)

Aboshi *et al.* (1979) developed the circular sliding surface method for evaluation of the stability using circular failure surfaces (Fig. 9) and a composite shear strength. The composite shear strength is determined based on a proportionate average of soil strength and stone column strength for a given area replacement ratio and stress concentration ratio (Aboshi *et al.* 1979).

The composite shear strength determined is also typically used in conjunction with the Ordinary Method of Slices, to determine the stability of the stabilized ground (Enoki 1991).

2.6 Deep Soil Mixed Piled Embankment

The stability of soft ground improved with deep soil mixed piles is often analyzed using a short term, undrained analysis because the shear strength of the deep mixed piles and the soil between piles generally increase over time. A composite or weighted average, undrained shear strength is used to evaluate slope stability for ground improved with deep mixed piles, assuming complete interaction between the stiff piles and the surrounding soft soil (Broms and Boman 1979). Embankment stability is typically analyzed assuming a circular shear surface as shown in Fig. 10.

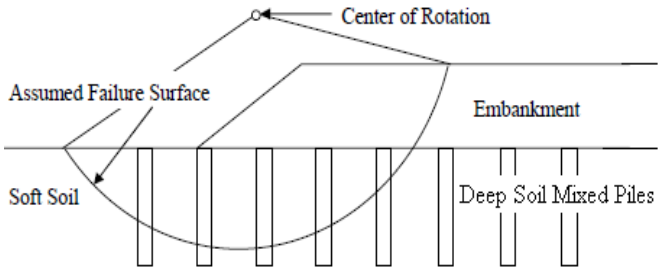

Figure 10. Circular sliding surface (after Broms and Boman 1979)

3 Case Histories

Case 1: Embankment on PVD Improved Ground

Indraratna *et al.* (1994) presented a case history of a full scale embankment raised on soft marine clay (Muar clay), stabilized with vertical band drains. The total height of the embankment upon completion was 4.75 m and was constructed over a period of four months. The embankment fill consisted of granitic residual soil compacted to a unit weight of 21kN/m^3. Pre-fabricated vertical drains (PVDs) of maximum length 18.0 m were installed underneath the embankment in a triangular pattern at spacing of 1.30 m. The drains consisted of polyolefine cores of rectangular cross section of size 95 mm x

4 mm with 24 channels. The sides of the drain were perforated with 0.2 mm diameter holes at 2 mm centres. Fig. 11 shows the cross section through the centre of the embankment.

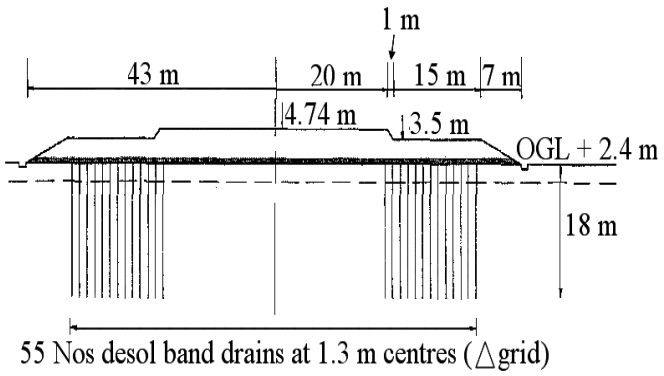

Figure 11. Cross section through centerline of embankment with vertical drains (after Indraratna *et al.* 1994)

The soil profile at the site consisted of top 2.0 m thick weathered crust overlying 16.5 m thick layer of soft silty clay. The soft silty clay is further divided into an upper very soft layer and lower soft silty clay. Below the lower clay lies a 0.3 m – 0.5 m thick peaty soil followed by a stiff sandy clay that ends at a dense sand layer at approximately 22.5 m below ground level. A fairly consistent unit weight of 15 – 16 kN/m^3 of the clay with depth was reported, except for the top most crust, where the unit weight approached 17 kN/m^3. The field permeability varied from 1 – 2 x 10^{-9} m/s with increasing depth within the soft clay layer. The undrained vane shear strength was found to have a minimum value of about 8 kPa at a depth of 3 m, and this increased approximately linearly with depth.

Extensive instrumentation was carried out for the soft clay foundation for monitoring the lateral movements (with the help of inclinometers) and vertical movements (with the aid of extensometers and settlement gauges) along with the development of excess pore water pressures (with the aid of pneumatic piezometers). A numerical analysis was also performed using the finite element code CRISP, to investigate the performance of the embankment and the underlying soft clay.

Fig. 12 shows the time-dependent pore pressure variations along the centerline of the embankment monitored by pneumatic piezometers located within the zone of influence of the vertical drains. A reasonable agreement between the finite element results and field data was observed upto an elapsed time of 100 days for the piezometer located at 13.6 m below ground level. Beyond 100 days of elapsed time, the finite element results underestimate the excess pore pressures due to retarded efficiency of the vertical drains with time (caused probably because of partial clogging of the drain perforations).

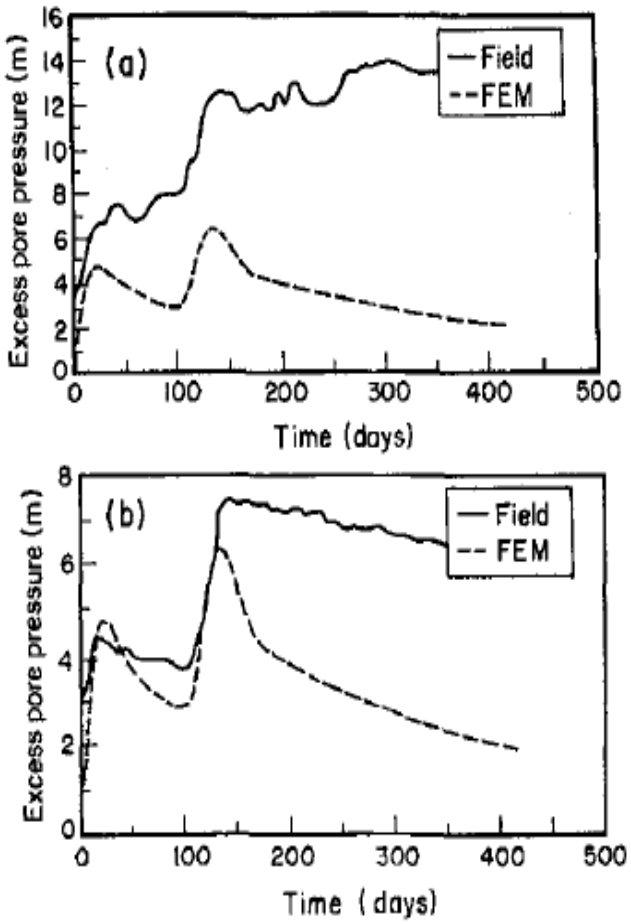

Figure 12. Variation of measured and calculated excess pore pressure with time at embankment centerline for piezometers located at (a) 9.1 m below ground level; and (b) 13.6 m below ground level (from Indraratna *et al.* 1994)

Fig. 13 shows the surface settlement profiles corresponding to time periods of 45 days and 413 days. The results of the finite element analysis with non-zero excess pore pressure dissipation at drains coincide fairly well with the field measurements at any time of measurement. At the initial stages, the results of the finite element analysis with perfect drains over predict the settlements but with passage of time, they begin to match fairly well with the measured settlements. Heaving of the ground (of the order of 100 mm) was also observed in the region immediately beyond the embankment toe (43 m from the centerline). The maximum measured settlement at the embankment centerline was about 1200 mm corresponding to a time period of 413 days.

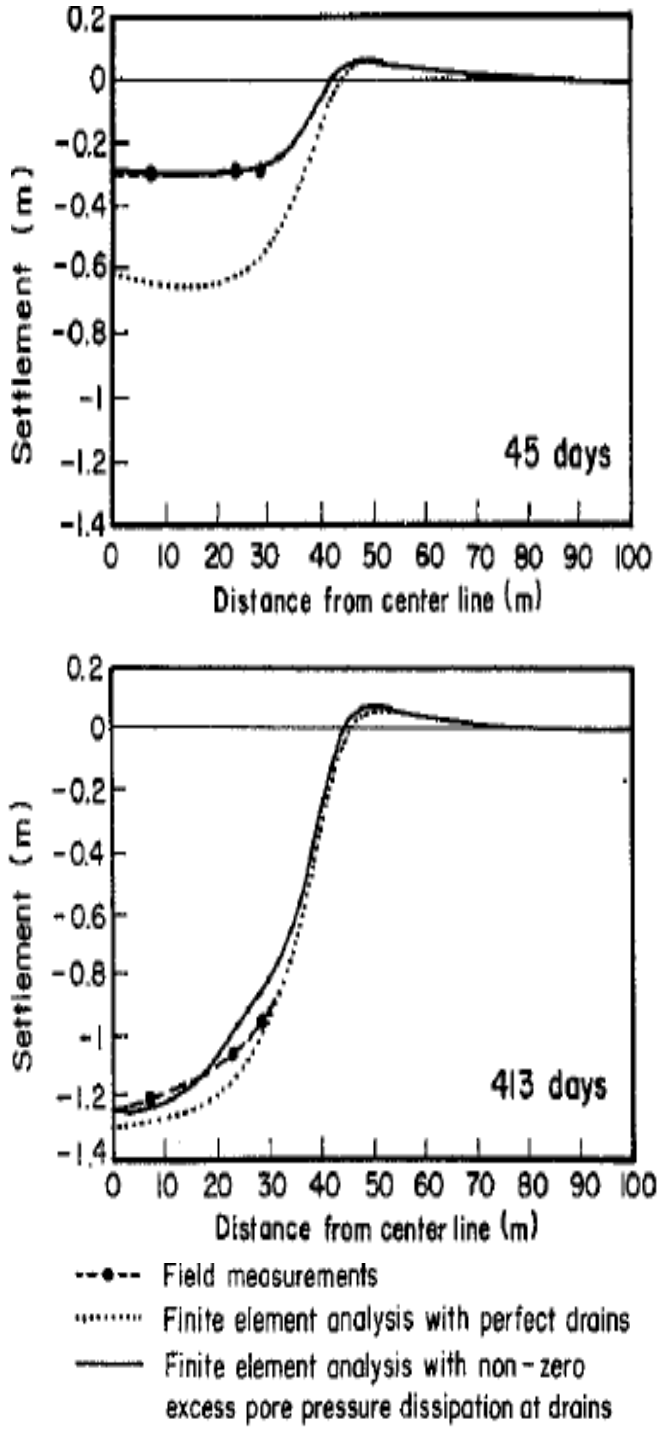

Figure 13. Surface settlement profiles at selected time periods (from Indraratna *et al.* 1994)

Fig. 14 depicts the variations of in-situ lateral displacements with time corresponding to inclinometer location at 23 m from the embankment centerline. These lateral displacements were considered as incremental or creep, due to subtraction of the initial lateral movement due to surcharge, from the total lateral displacement observed at any given time. Maximum lateral displacements at any given time were measured within the upper soft clay layer (5 m depth), whereas, within the deeper (stiffer deposits), lateral displacements were expectedly curtailed.

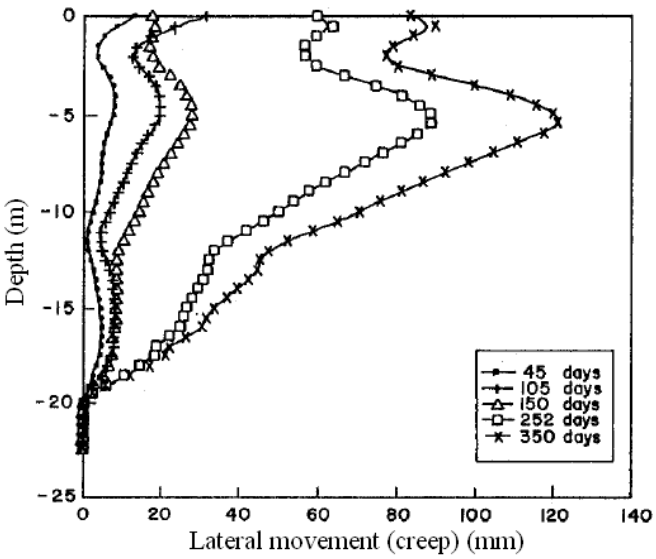

Figure 14. Development of lateral movements at various time periods (from Indraratna *et al.* 1994)

Case 2: Basal Reinforced Embankment

Chai and Bergado (1993) presented a case history of a geogrid reinforced embankment constructed over soft Muar clay with vertical band drains (without filter) in the foundation. The embankment was constructed with a base width of 88 m and length of 50 m, initially to a fill thickness of 3.9 m. 15 m wide berms were then constructed on both sides and the embankment raised to a final fill thickness of 8.5 m. The geometry and field instrumentation are shown in Fig.15. A cohesive - frictional soil consisting of decomposed granite with consistency of sandy clay was used as fill material for the embankment.

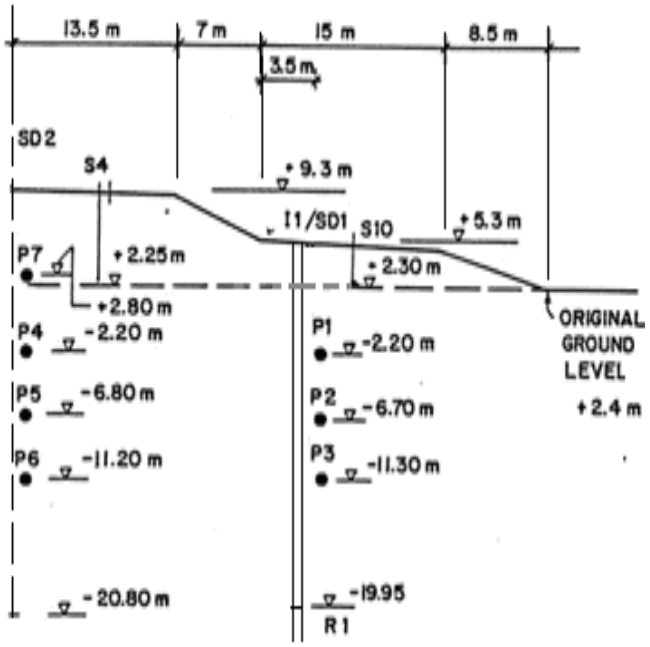

Figure 15. Geometry and instrumentation of embankment (after Chai and Bergado 1993)

The soil profile at the site consisted of a weathered crust at the top 2.0 m, underlain by about 5 m of very soft silty clay. 10 m of soft clay lies below this layer which in turn is underlain by about 0.6 m of peat. A thick deposit of medium dense to dense clayey-silty-sand exists beneath the peat layer. Fig. 16 shows the index properties, initial void ratios, compressibility indices, maximum past vertical effective pressures, and permeabilities of the foundation soil.

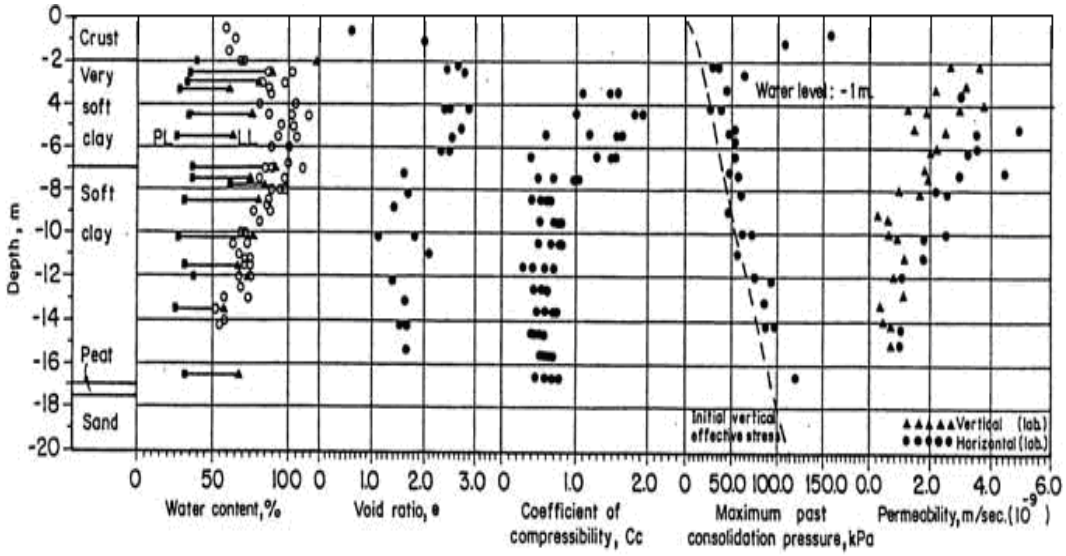

Figure 16. Geotechnical properties of Muar clay (from Chai and Bergado, 1993)

The vertical band drains were installed in a square pattern at 2.0 m spacing upto a depth of 20 m, to ensure that the estimated settlement could be obtained within the allowed construction period of 15 months (in other words, only for the purpose of accelerating the consolidation process). The width and thickness of the drains were 95 mm and 4 mm respectively, and consisted of 24 channels. The sides of the drain were perforated with 0.2 mm diameter holes. After installation of the vertical drains, two layers of geogrid were laid with vertical spacing of 0.15 m in a 0.5 m thick sand blanket having friction angle of 38^0, and placed at the base of the embankment to ensure a factor of safety of 1.3 during construction (Ting *et al.* 1989). The strength of the geogrid was 110 kN/m with a peak strain of 11.2%. The behaviour of the soft foundation soil was described by the modified Cam clay model (Roscoe and Burland, 1968) and the consolidation process of the soft clay was simulated by the coupled consolidation theory (Biot, 1941). In the finite element method, two different soil-reinforcement interaction modes, direct shear and pull out, were considered.

Fig. 17 shows the variation of the excess pore pressure with elapsed time for a piezometer point 4.5m below the ground surface and on the embankment centerline. With reference to Fig. 17, "Higher permeability" implies that the vertical hydraulic conductivity is twice that of "Lower permeability", while "Varied permeability" implies that the initial values are similar to "Higher permeability" but vary with void ratio following the equation.

$$k = k_0 . 10^{-(e_0 - e)/C_k} \qquad (1)$$

where k_0 is initial hydraulic conductivity, e_0 is initial void ratio, k is current hydraulic conductivity, e is current void ratio, and C_k is a constant ($C_k = 0.5e_0$, Tavenas *et al.* 1983).

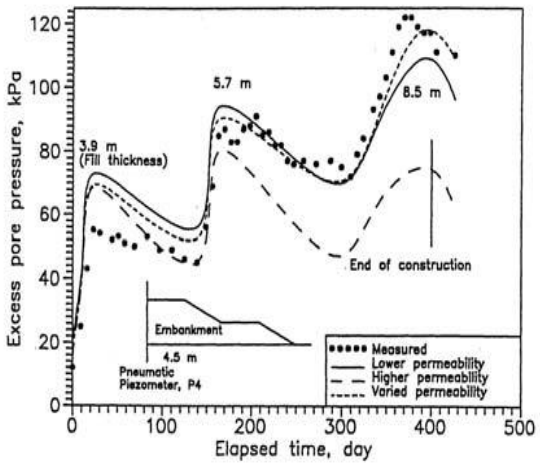

Figure 17. Excess pore pressure versus elapsed time (from Chai and Bergado 1993)

The finite element analyses, especially the "Varied permeability" analysis simulated both excess pore pressure build up as well as dissipation, for the stage constructed embankment well. However, at an early stage of embankment construction (3.9 m fill thickness), the estimated pore pressures were higher than the measured ones due to the

adoption of a lower value of permeability (than the actual) in the finite element analysis.

Fig. 18 presents the predicted and measured surface settlement profiles. The predicted settlements based on the varied permeability assumption were in good agreement with the measured settlements. At an early stage of embankment construction (3.9 m fill thickness), the finite element analysis yielded larger settlement at the zone near the embankment toe, than at the center of the embankment but in agreement with field measurements. This was because the zone near the embankment toe had high shear stresses that caused lateral yielding of the soil, thus resulting in larger settlement. The maximum measured settlement at the embankment centerline was about 1500 mm corresponding to fill thickness of 8.5 m at elapsed time of 398 days. A maximum heave of about 250 mm was reported beyond the toe of the embankment.

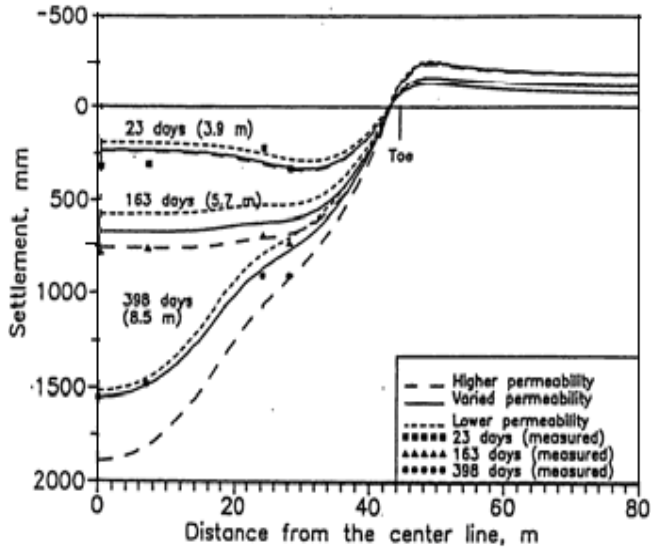

Figure 18 Surface settlement profile
(from Chai and Bergado 1993)

Fig. 19 shows a comparison between the finite element results and the measured lateral displacements. At an early stage of embankment construction (3.9 m fill thickness), the predicted values are slight overestimates while at the end of embankment construction (8.5 m fill thickness) the predicted values underestimate the lateral displacements. Further, the change in shape of the lateral displacement profile at 2.0 m depth was not predicted by the finite element results. This variation of the lateral displacement coincided with the results of settlement and thus showed that the consolidation process of the soft foundation soil at very early stage of embankment construction was not properly simulated by the finite element analysis. Maximum lateral displacements occurred within the very soft clay layer (5 m depth) and decreased thereafter with increased depth.

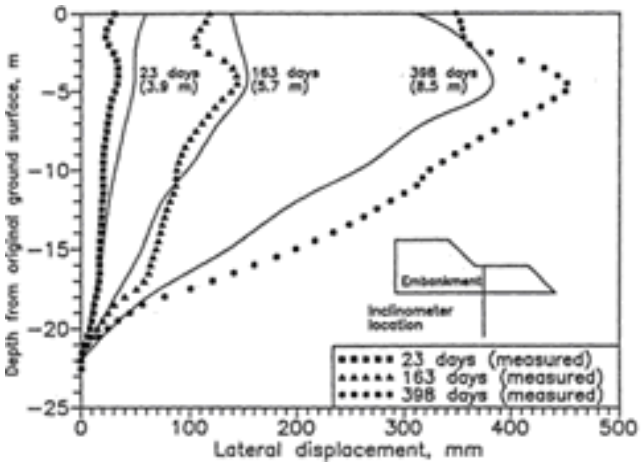

Figure 19. Lateral displacement profile
(from Chai and Bergado 1993)

Fig. 20 compares the estimated reinforcement tension force distributions for different fill thicknesses. At the early stage of embankment construction (3.9 m fill thickness), high tensile force developed near the embankment toe at the location of the high shear stress zone. However, after the construction of 15 m wide berms on both sides of the embankment and due to the consolidation effect, the tension force in the reinforcement increased under the center of the embankment but decreased under the berm. The calculated maximum tension force in each layer of geogrid at the end of construction (8.5 m fill thickness) was 13 kN/m (in total 26 kN/m for two layers of geogrid), equivalent to an axial strain of 2%. The calculated maximum tensile force in each layer of geogrid increased to 20 kN/m, three years after the final construction, thus indicating that the maximum tensile force in each layer of geogrid increases during the consolidation process of the soft foundation soil.

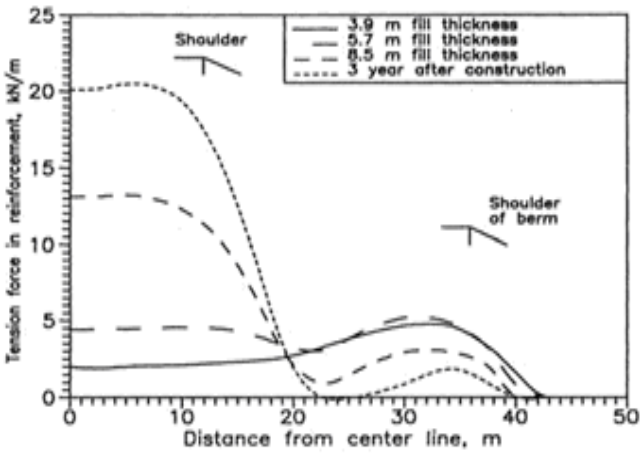

Figure 20. Tension in reinforcement
(from Chai and Bergado, 1993)

Case 3: Piled Embankment

Chen *et al.* (2010) presented a case history of a pre-stressed tube pile-supported highway embankment constructed over 20 m thick soft clay of very low strength and high compressibility. Pre-stressed tube piles were adopted to improve the load carrying capacity of the soft ground and to withstand the load from a 126 m long test embankment. The embankment was 6.0 m high with a crown width of 26 m and side slopes of 1(V):1.5(H). The embankment fill consisted of gravel mixed with clayey soil with a friction angle of 32^0 and an average unit weight of 21 kN/m^3. The length of the prestressed tube piles was 20 m and the piles were driven down to the firm strata. The outer diameter of the pile was 0.4 m, thickness of the concrete annulus was 5 cm. All the piles were installed in a square pattern. The embankment was raised to the height of 6 m over a period of 65 days. Fig. 21 shows the cross section and plan views of the test section, arrangement of piles and the instrumentation carried out.

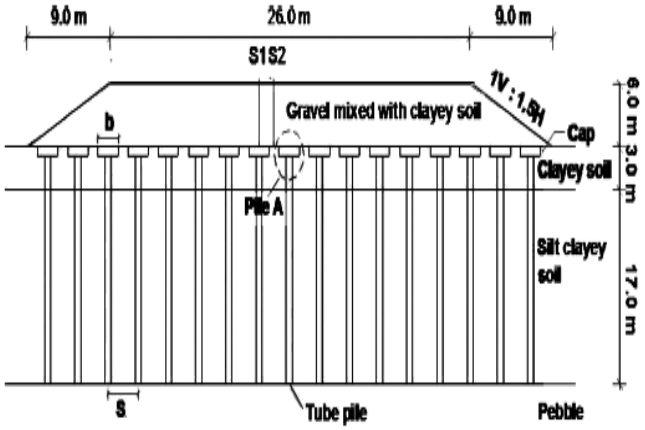

Sectional view of piled embankment

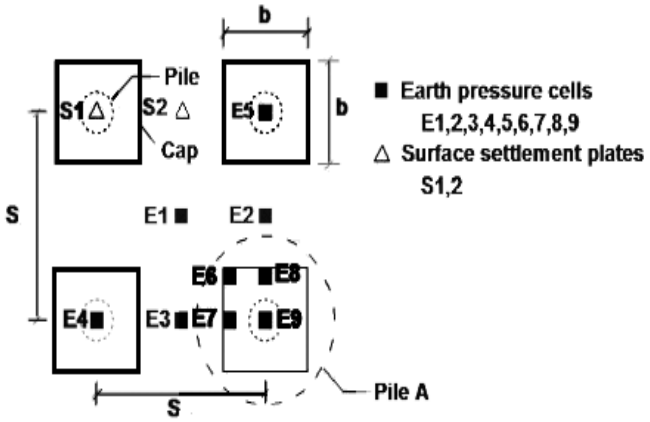

Plan view of tube piles in square layout along with location of various instrumentation points

Figure 21. Cross section & plan view of piled embankment, field instrumentation and pile arrangement (after Chen *et al.* 2010)

Monitoring was carried out in three sections of the embankment, section K18+223 (defined as G1 section), section K18+253 (defined as G2 section) and section K18+283 (defined as G3 section) respectively. The detailed information of these test sections are listed in Table 1. The soil profile at the site consisted of a top 3 m thick crust of low compressible silt (ML) underlain by 16 to 17 m thick layer of soft, low compressible clay (CL). The CL layer had high water content, poor permeability and low shear strength. 15 to 17 m thick pebble (GM) layer lies below the CL layer. The ground water table was reported to be at a depth of 0.5 m below the ground surface.

Fig. 22 shows the average earth pressures acting on the pile caps and the soil surfaces measured by the earth pressure cells, defined as P_p and P_s respectively. During the first 20 days, the embankment reached a height of 1.5 m, and the earth pressures on the pile caps and the soil surfaces increased with fill height. The increase in earth pressures on the pile caps was sharp when compared to that on the soil surface. The earth pressures at-

Table 1. Detailed information of various test sections in piled embankment (from Chen et al. 2010)

Test section	*H* (m)	*d* (m)	*L* (m)	*S* (m)	Cap shape	*a* (m)	Arrangement of piles
G1	6.0	0.4	20	2.5	Square	1.3	Square
G2	6.0	0.4	20	3.0	Square	1.6	Square
G3	6.0	0.4	20	2.0	Square	1.0	Square

H is the embankment height; *a* is the width of the pile cap; d_0, L and S are the diameter, length, and spacing of the piles, respectively.

tained peak values at about 25 – 60 days and then decreased to relatively steady values at 80 days and thereafter. The decrease of the earth pressures on the soil was attributed to the consolidation of the soil as well as the soil arching developed in the fill.

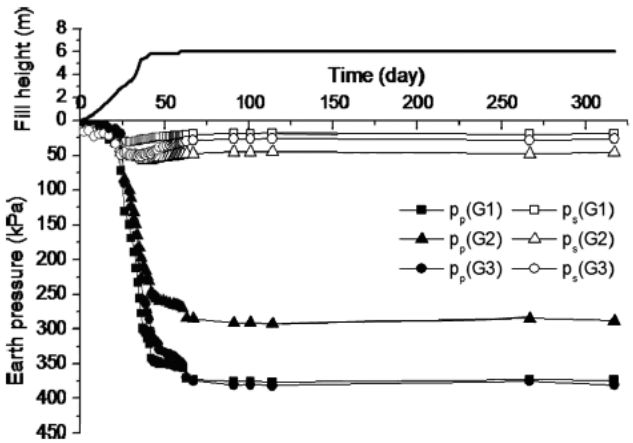

Figure 22. Measured earth pressures at test sections (from Chen *et al.* 2010)

When the fill height reached 6.0 m at the end of the embankment construction, the pressures on the top of the pile caps in G1 and G3 sections were about 380 kPa, while that measured in G2 section was 288 kPa. The lower steady value of P_p in G2 section was attributed to the larger net spacing of the piles in G2 section (3.0 m) when compared to G1 (2.5 m) and G3 (2.0 m) sections. The pressures on the soil between the piles were much smaller than those measured on the piles. Majority of the embankment load was carried by the piles due to which the soft soil beneath the embankment was subjected to a relatively much smaller load. This shows that there was a load transfer from the soil to the pile as a result of soil arching in the embankment fill. The steady earth pressures after the end of the embankment construction were due to the fact that the piles were founded on a firm layer, and also indicate completion of the soft soil consolidation after the filling.

Fig. 23 presents the measured settlements both on the pile cap (surface settlement marker S1) and on the soil surface between the piles (settlement marker S2). The settlements increased with fill height and most of the total settlements occurred during the period of embankment construction itself, with small subsequent settlements thereafter due to soil consolidation. The measured total settlements in G2 section (having 3.0 m pile spacing) were larger than those measured in other sections, while the data obtained in G3 section (having 2.0 m pile spacing) was the smallest, thus indicating that the pile spacing effects the settlements, i.e., closer the pile spacing, smaller was the settlement of the pile cap as well as the soil surface between the piles.

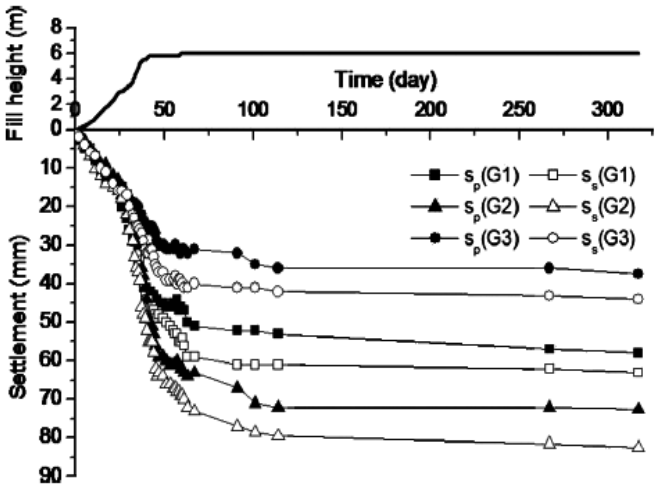

Figure 23. Measured settlements at test sections (from Chen *et al.* 2010)

At the end of the monitoring period, the maximum measured settlements were only 72 mm and 82 mm at the pile cap and at the soil surface, respectively. Similar to the total settlements, the differential settlements (i.e., difference in settlement at top of pile cap and soil surface) also increased with fill height. However, no increase in differential settlement was observed after the embankment construction. The maximum measured differential settlement was only 10 mm.

Case 4: Basal Reinforced Piled Embankment

Liu et al. (2007) presented a case history of a geogrid reinforced piled highway embankment constructed with a low area improvement ratio of 8.7% over soft clay in the northern suburb of Shanghai. The embankment was 5.6 m high and 120 m long with a crown width of 35 m and side slopes of 1(V):1.5(H). The fill material consisted of pulverized fuel ash with cohesion of 10 kPa, a friction angle of 30^0, and an average unit weight of 18.5 kN/m^3. Extensive field instrumentation was performed to obtain data related to the contact pressures acting on the pile and soil surface, pore water pressures, settlements and lateral displacements. The case history was back analyzed by carrying out three-dimensional (3D) fully coupled finite element analysis using finite element software ABAQUS (HKS 1997). Fig. 24 shows the cross section of the test embankment with complete details of the instrumentation.

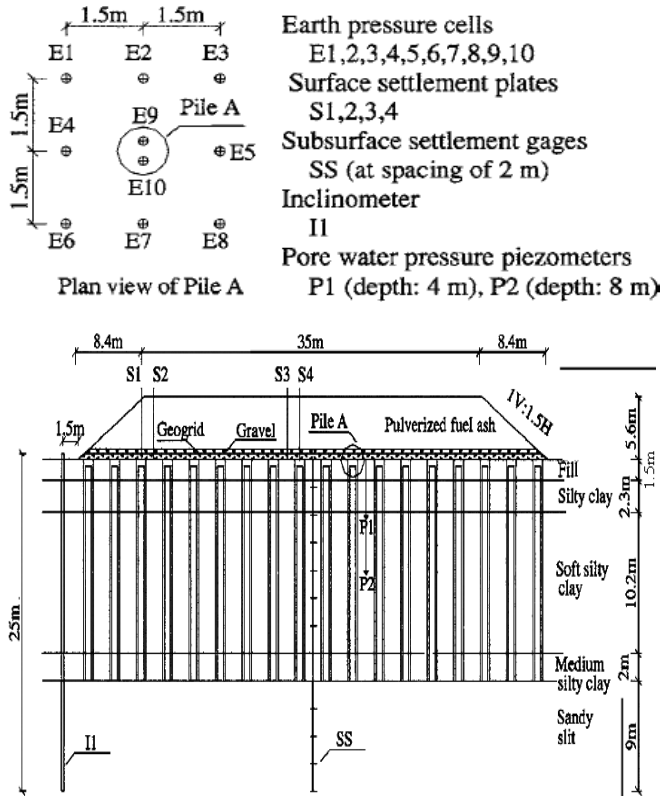

Figure 24. Plan and cross section of instrumented embankment (after Liu et al. 2007)

The embankment was supported by cast-in-place annular concrete piles formed from a low-slump concrete with a minimum compressive strength of 15 N/mm^2. The annular concrete piles were 16 m long and were founded on a relatively stiffer sandy silt layer. The outer diameter of each pile was 1.008 m and the thickness of the concrete annulus was 120 mm. The annular concrete piles were installed in a square pattern at a centre to centre spacing of three times the pile diameter (i.e., 3 m). A single layer of biaxial polypropylene grid (TGGS90-90) was sandwiched between two 0.25 m thick gravel layers to form a 0.5 m thick composite-reinforced bearing layer. The tensile strength in both directions (longitudinal and transverse directions) of the geogrid was 90 kN/m and the maximum allowable tensile strain was 8%. The embankment was constructed to a height of 5.6 m over a period of about 55 days.

The soil profile at the site consisted of a 1.5 m thick coarse grained fill overlying 2.3 m thick deposit of silty clay which in turn overlies 10.2 m thick soft silty clay layer. Below the soft silty clay layer was 2.0 m thick medium silty clay layer followed by sandy silt layer. The ground water level was reported to be at a depth of 1.5 m below the ground surface. Fig. 25 shows the variation of water content and vane shear strength up to a depth of 24 m below the ground level. The soft silty clay layer had low to medium plasticity with a liquidity index of 1.2 along with water content ranging between 40 and 50%, close to the liquid limit. The uppermost coarse-grained fill layer had relatively high preconsolidation pressure, in comparison with the underlying soft silty clay, which was normally consolidated or lightly overconsolidated. The undrained shear strength of the soft silty clay layer measured by the field vane had a minimum value of about 10 kPa at a depth of 3.8 m and increased approximately linearly with depth.

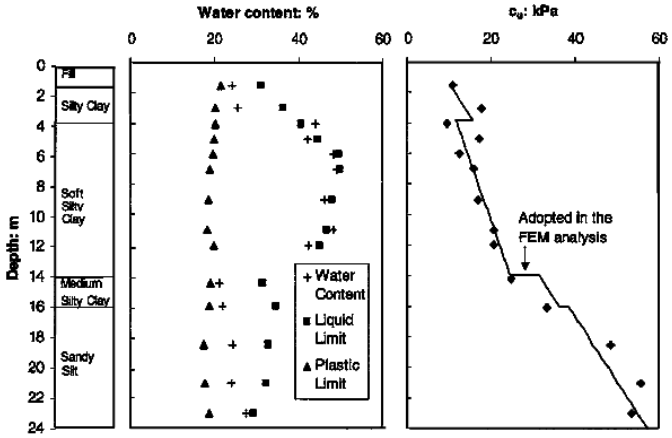

Figure 25. Soil profile and properties (after Liu *et al.* 2007)

Figs. 26 and 27 show the measured vertical pressures acting on the soil surface between the piles as well as that on top of the pile, respectively. A marked reduction in actual stress applied to the foundation soil was observed. When the embankment was built to its final height of 5.6 m, giving rise to a pressure of 104 kPa, the measured pressures acting on the soil surface increased by 31–58 kPa, i.e., by only 0.3 to 0.6 times the embankment load. On the other hand, the pressure acting on the pile head increased to 674 kPa, i.e., by 6.5 times the embankment load. Thus, much of the applied pressure from the embankment was taken by the piles and very little pressure was transferred to the soft soil between the piles.

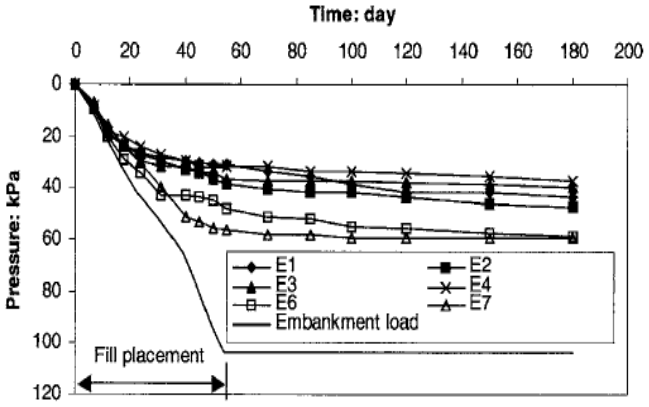

Figure 26. Measured earth pressure acting on soil surface between the piles (from Liu *et al.* 2007)

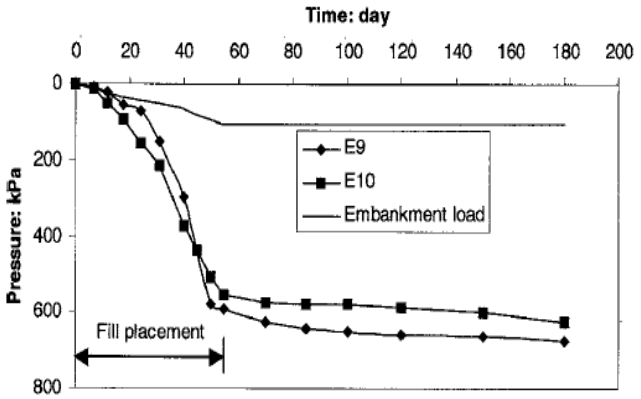

Figure 27. Measured earth pressure acting on top of pile (from Liu *et al.* 2007)

Fig. 28 shows the measured and predicted variations in the piezometric levels with time in the soft silty clay at 4.0 m depth (P1, z = 21 m) and 8.0 m depth (P2, z = 17 m) below the centre of the embankment. The bottom of the sandy silt layer was considered as the reference datum. Both the measured and predicted results illustrate an increase in excess pore pressures during the period of construction due to increase in surcharge load of 104 kPa. However, the increases of P1 and P2 were only about 11 kPa and 14 kPa respectively. This small increase in pore pressure was due to load transfer from the soft clay to adjacent piles as a result of soil arching as well as some dissipation of pore water pressure during construction. Once again, the piles carried the major part of the embankment load, while the soft clay beneath the embankment was subjected to a very small load. Thus small excess pore pressures were induced at piezometers P1 and P2 in the soft clay.

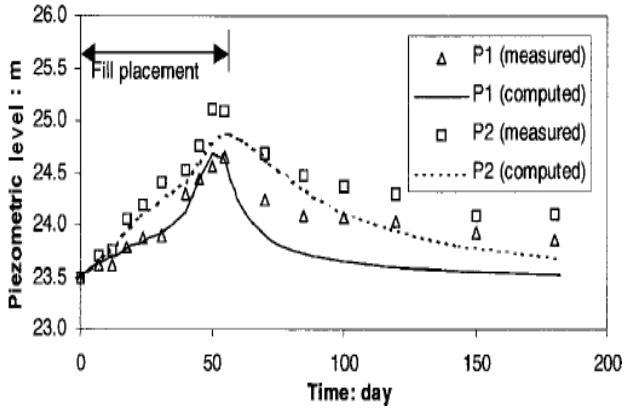

Figure 28 Measured and predicted variations of piezometric level below the embankment centerline (from Liu *et al.* 2007)

Figs. 29 and 30 depict the measured and predicted settlements on the pile heads (measured by surface settlement markers S1 and S4) and on the soil surface between the piles (measured by S2 and S3), respectively.

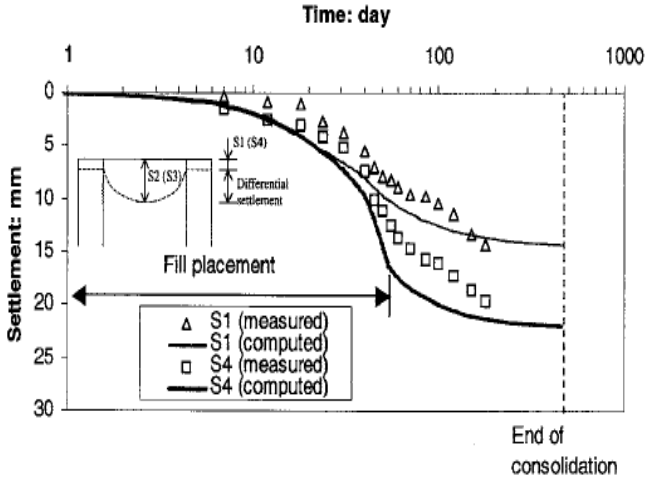

Figure 29. Measured and predicted surface settlements at the pile head (from Liu *et al.* 2007)

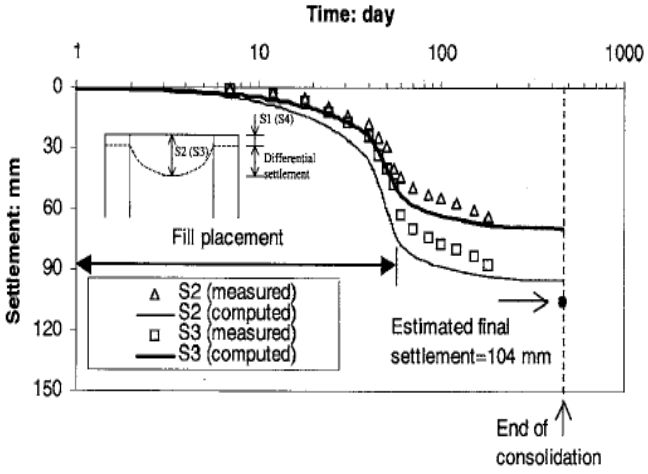

Figure 30. Measured and predicted surface settlements at the soil surface (from Liu *et al.* 2007)

The computed settlements agreed reasonably well with field measurements with maximum settlement occurring at the midpoint between the piles. At the end of embankment construction, the maximum measured settlements were only 14 mm and 63 mm at the pile head and at the soil surface, respectively. At the end of the monitoring period (i.e., 180 days after commencement of embankment construction), the maximum measured settlements increased by only 5 mm and 24 mm at the pile head and at the soil surface respectively, due to consolidation. The final settlement was estimated to be 104 mm (Fig. 30) based on the hyperbolic method proposed by Tan *et al.* (1991). As the soil settlement between the piles was considerably larger than the pile settlement, down-drag of piles was inevitable and the same may be considered in future designs.

Fig. 31 presents the finite element computed tensile force developed in the geogrid around pile A (Fig. 24) at the end of embankment construc-

tion. The maximum computed tensile force developed in the geogrid was 20 kN/m, about 22% of the tensile strength of the geogrid (90 kN/m). A sharp reduction of tensile force in the geogrid occurred from the edge of the pile to the centre, due to sharp change in the settlement near the edge of the pile. As a result, maximum tensile force computed in the geogrid was near the pile edge. Unfortunately, no field measured tensile force data was available for comparison with the computed values.

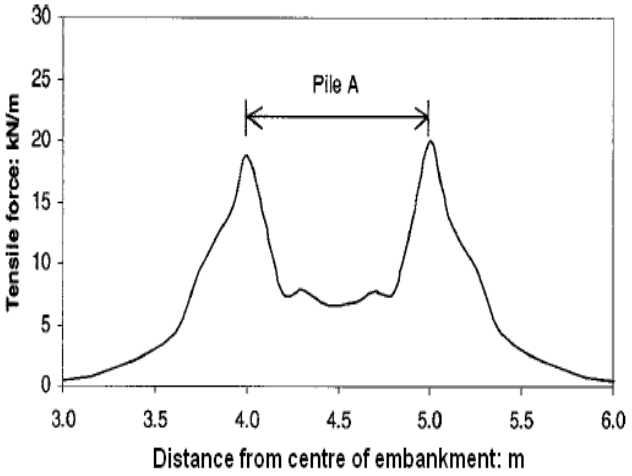

Figure 31. Computed tensile force in geogrid around pile A at end of embankment construction (from Liu *et al.* 2007)

Fig. 32 shows the measured and predicted lateral displacement profiles at inclinometer location I1 at 1.5 m from the toe of the embankment (Fig. 24). 3D finite element simulation reasonably captured the shape of the lateral displacement profiles but significantly over-predicted the magnitude of the lateral displacements due to the use of an isotropic homogeneous soil model, rather than a realistic anisotropic one. The maximum lateral displacements measured at 4 m depth in the upper silty clay layer were 4 mm and 10 mm corresponding to fill heights of 2.8 m and 5.6 m respectively.

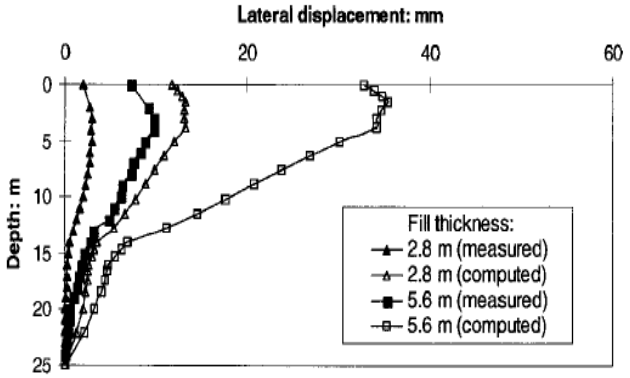

Figure 32. Measured and predicted lateral displacement profiles (from Liu *et al.* 2007)

Case 5: Embankment on Stone Column Treated Ground

Oh *et al.* (2007) presented a case history of a highway embankment constructed over soft estuarine clay with high sensitivity and low undrained shear strength. The embankment was divided into three sections, section 1 with no stone columns, section 2 with stone columns at 2 m spacing, and section 3 with stone columns at 3 m spacing. The embankment was constructed in two stages, each stage consisted of a fill height of 2 m and thus the final height of the embankment was 4 m. The width of carriageway was 4 m and the side slopes of the embankment were 1(V):2(H). The stone columns constructed in a square pattern with column diameter of 1 m & column length of 14 m, were installed using vibro-replacement technique. Fig. 33 shows the geometry of the embankment over stone column treated ground.

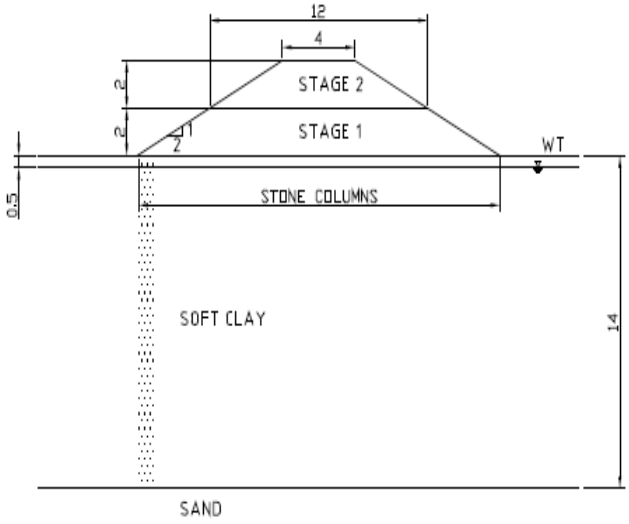

Figure 33. Geometry of the embankment over stone column treated ground, all dimensions in *m* (after Oh *et al.* 2007)

The soil profile at the site consisted of 14 m thick very soft to soft organic clay layer overlying moderately dense to dense sandy sediment strata, with stiff-hard clay/silty clay on either side of the sand strata. The groundwater table was reported to be at a depth of 0.5 m below the ground surface. Fig. 34 shows the variation of natural moisture content, liquid & plastic limits, and undrained shear strength, with depth. The natural moisture content varied between 60% and 120% and was greater than the liquid limit of the soil. The liquidity indices were in the range of 1.5 to 2.5, indicating high sensitivity. The undrained shear strength varied with depth ranging from very low values of 5 kPa to 20 kPa. Based on the results of oedome-

ter tests, the compressibility of the soft clay ranged from 0.5 to 3.5 m^2/MN while the coefficient of consolidation varied from 0.2 to 0.3 m^2/year.

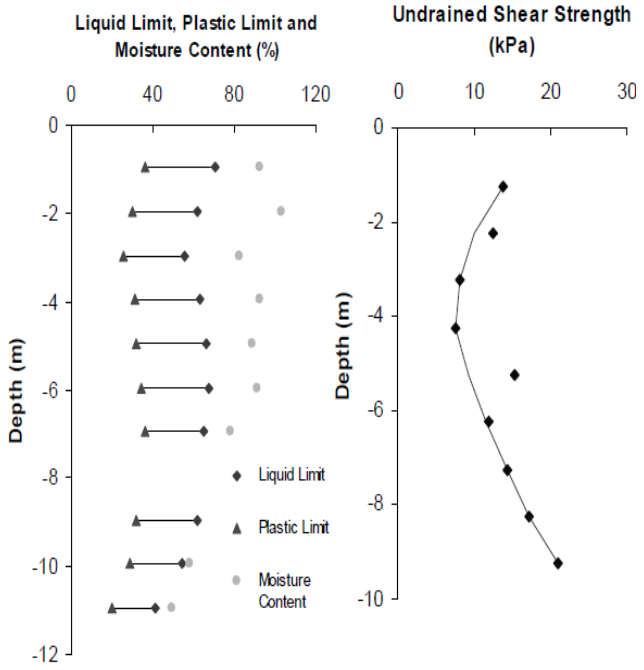

Figure 34. Variation of natural moisture content, liquid & plastic limits, and undrained shear strength, with depth (from Oh *et al.* 2007)

Field instrumentation in the form of settlement gauges, horizontal profile gauges and inclinometers were installed during construction of the embankment. The settlement gauges were installed at the embankment centerline to monitor the vertical settlement while the horizontal profile gauges were installed across the base of the embankment to record the horizontal settlement profile of the embankment. Inclinometers were installed at the toe of the embankment to monitor the lateral displacements.

Figs. 34, 35 and 36 show the measured settlement profiles corresponding to untreated embankment, embankment with stone columns at 3 m & 2 m spacing, respectively, at different monitoring periods. The settlement of the embankment increased with time for both untreated as well as stone column treated case. The maximum measured settlements were about 520 mm, 495 mm and 390 mm for untreated, 3 m spaced & 2 m spaced stone column treated ground, respectively. The reduction in settlement was 5% and 25%, of the settlement for untreated case, corresponding to 3 m and 2 m spaced stone columns, respectively. Thus, installation of closely spaced stone columns reduced the amount of settlement.

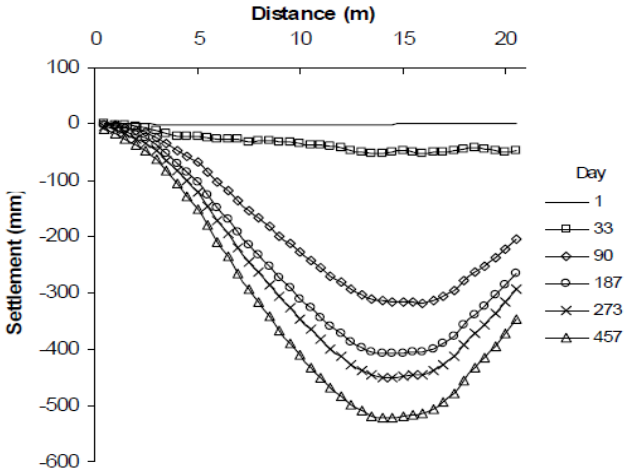

Figure 34. Settlement profiles for embankment without stone columns (from Oh *et al.* 2007)

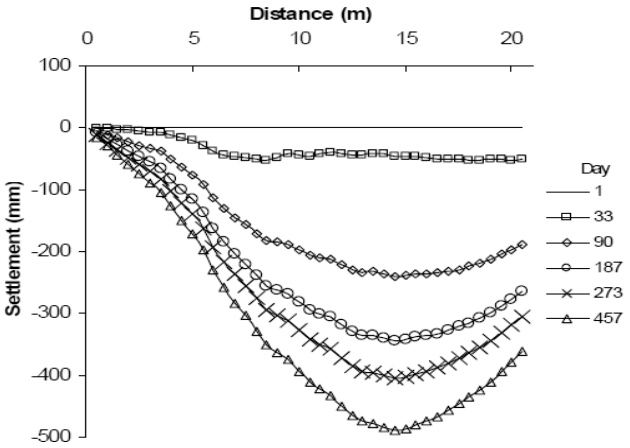

Figure 35. Settlement profiles for embankment treated with stone columns at 3 m spacing (from Oh *et al.* 2007)

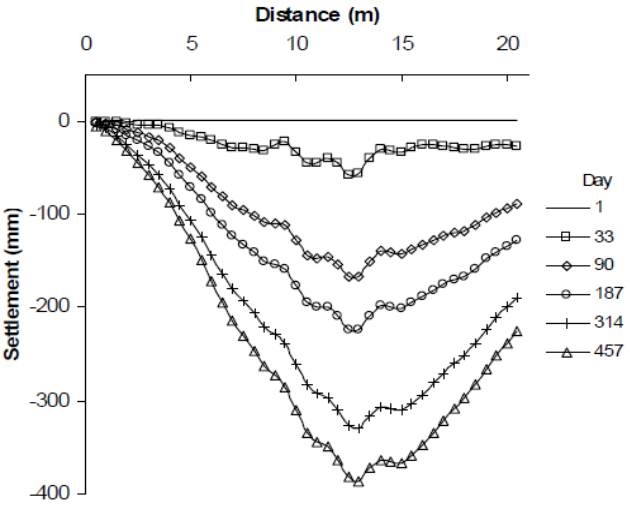

Figure 36 Settlement profiles for embankment treated with stone columns at 2 m spacing (from Oh *et al.* 2007)

Fig. 37 presents the measured lateral displacement profiles based on inclinometer results, immediately after embankment construction and at 230 days after completion, for untreated as well as 2 m & 3 m spaced stone column case. The maxi-

mum lateral displacement was 77 mm measured at a depth of about 3 m within the sensitive soft clay layer, 230 days after completion of an untreated embankment. Installation of stone columns at 2 m spacing reduced the amount of lateral displacement approximately by half, when compared to the embankment with no ground improvement. The lateral displacement of the embankment with stone columns at 3 m spacing was slightly higher when compared to the one with 2 m spacing. Thus, installation of stone columns beneath the embankment reduced the lateral displacement, which further reduced with decreased column spacing.

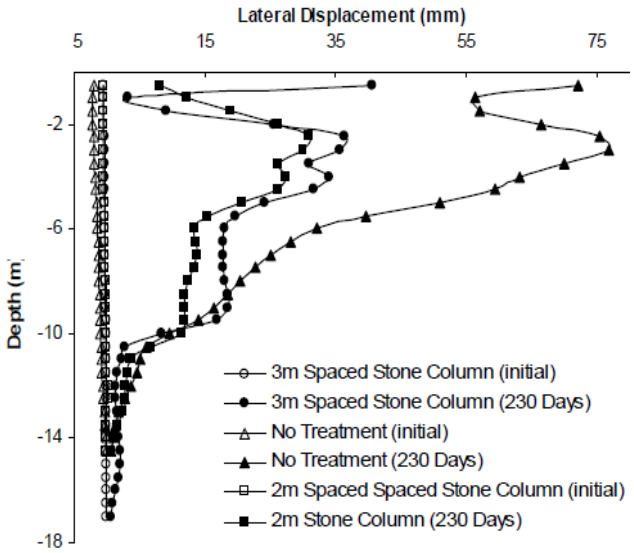

Figure 37. Lateral displacement profiles (from Oh et al. 2007)

Case 6: Embankment on Deep Cement Mixed Piles

Bergado *et al.* (2009) presented a case history of a full scale 5 m high test embankment constructed over soft Bangkok clay improved using deep cement mixed (DCM) and stiffened deep cement mixed (SDCM) piles. Jet mixing method with jet pressure of 22 MPa was employed to install the DCM pile and SDCM piles in-situ, for improvement of the foundation subsoil. The deep mixing piles were installed at 2.0 m spacing in a square pattern. The water-cement ratio of the cement slurry and the cement content employed for the construction of deep mixing piles were 1.5 and 150 kg/m3 of soil, respectively. The diameter and length of each pile was 0.6 m and 7.0 m respectively and the piles were installed down to the bottom of the soft clay layer as shown in the section view of the embankment (Fig. 38). A pre-stressed concrete core pile of square section with 0.22 m width and 6.0 m length was inserted at the center of the soil-cement slurry to form the SDCM pile. The monitoring instruments were installed 30 days after the installation of the DCM and SDCM piles and thereafter, the full scale test embankment was constructed. The embankment was constructed within 30 days using weathered clay and silty sand as fill materials with compacted unit weights of 17 and 16 kN/m^3 respectively.

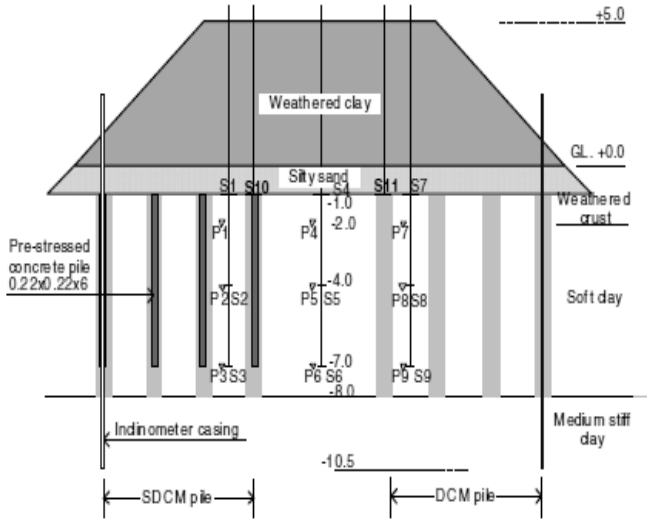

Figure 38. Section of instrumented test embankment supported by SDCM and DCM piles (after Bergado *et al.* 2009)

The soil profile at the site consisted of a top 2.0 m thick weathered crust of dark brown clay, underlain by a 6.0 m thick soft, highly compressible gray clay layer. Below the soft clay layer lies 2.0 m thick medium stiff clay layer. The groundwater table was reported to fluctuate seasonally with an average value of 1.5 m below the ground level. Fig. 39 shows the variation of natural water content, w_N, liquid & plastic limits, and undrained shear strength with depth.

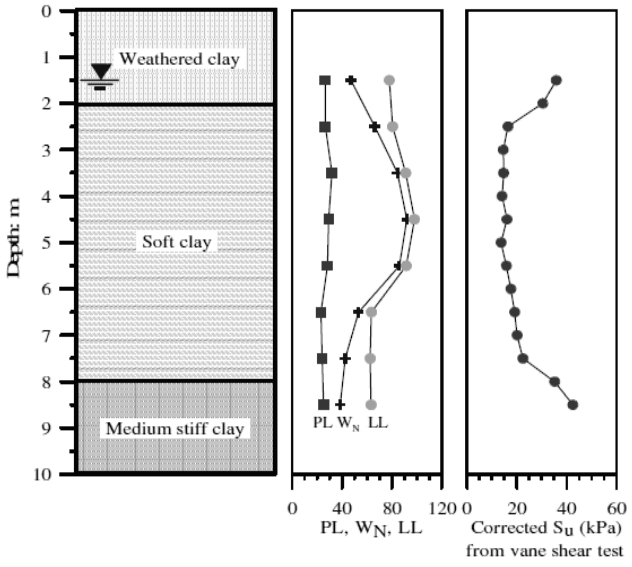

Figure 39. Variation of natural water content, liquid & plastic limits, and undrained shear strength, with depth (from Bergado *et al.* 2009)

Fig. 40 shows the settlements on the top of the SDCM pile, DCM pile, surrounding clay of SDCM pile, surrounding clay of DCM pile and on the surface of unimproved clay during and after construction, up to 570 days of full embankment loading. The settlements on the top of the SDCM pile, DCM pile, surrounding clay of SDCM pile, surrounding clay of DCM pile and on the surface of unimproved clay after the construction of the embankment were 97, 128, 118, 167 and 175 mm, respectively, and at 570 days after embankment construction were 161, 265, 250, 296 and 353 mm, respectively.

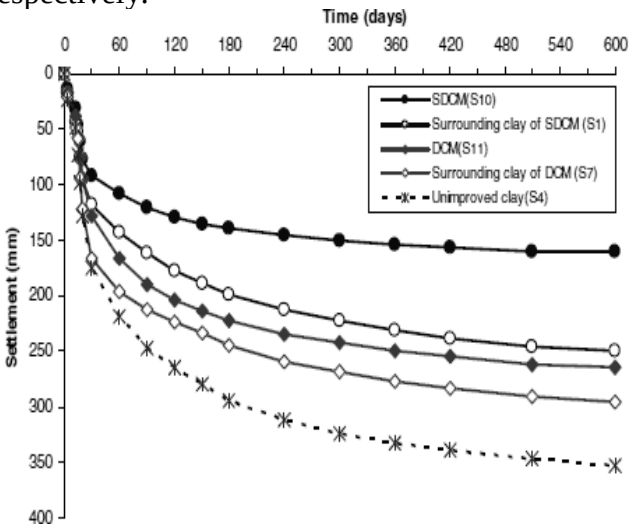

Figure 40. Surface settlements of pile and of surrounding clay (from Bergado *et al.* 2009).

Approximately, 50% of the total settlement occurred during the construction of the test embankment. The settlement of the clay surrounding the SDCM pile was smaller than that surrounding the DCM pile, which implies that the embankment load was transferred to the SDCM pile more efficiently than to the DCM pile. Moreover, the settlement of the SDCM pile was much less than that of the DCM pile and consequently, effected a settlement reduction of 40%. Thus, SDCM piles reduce the intensity of pressure on the surrounding soft ground which in turn reduces the settlement, leading to increased bearing capacity of the soft foundation ground.

4 Conclusions

A number of techniques are available for constructing stable embankments over soft ground. The final choice of adoption of a suitable technique depends on the in-situ conditions, embankment geometry, time constraints and the long term benefits. The stability of embankments over soft ground is generally analysed based on limit equilibrium analysis by assuming potential slip surfaces and identifying the one that gives the minimum factor of safety. In the case of piled embankments, the stability depends on the extent of development of soil arching within the embankment fill, while in the case of a basal reinforced piled embankment, it is a combination of soil arching and geosynthetic tension that affects the stability.

Six case histories of embankments constructed on soft ground using different techniques have been presented. Case 1 presents an embankment constructed on pre-fabricated vertical drain (PVD) improved ground. The PVDs helped in accelerating the consolidation process but over a period of time, the embankment experienced very large settlement accompanied by large lateral deformation of the subsoil. Case 2 descibes a basal (geogrid) reinforced embankment over soft clay. The geogrid reinforcement did not seem to have much effect on the stability of the embankment based on the small magnitude of mobilized tension, and further, the embankment faced problems similar to Case 1, i.e., large settlement and lateral deformation of subsoil.

Case 3 presents a piled embankment over thick soft clay. The piles carried majority of the embankment load as a result of soil arching developed within the embankment fill, and thus reduced the amount of load transferred to the surrounding soft clay. This in turn, led to a drastic reduction in settlement and improved the load carrying capacity of the soft ground. Case 4 illustrates a basal (geogrid) reinforced piled embankment over soft clay. Similar to Case 3, most of the applied load was carried by the stiffer piles with very small load transferred to the adjacent soft ground. Maximum tension in the geogrid developed near the pile edge with a minimum value between the piles.

Case 5 compares responses between untreated embankment and embankments treated with stone columns with 2 m & 3 m spacing over soft estuarine clay. The embankment treated with stone columns spaced at 2 m experienced least settlement as well as lateral deformation when compared to the values for embankment treated with 3 m spaced stone columns and the embankment with no ground improvement. Hence, installation of closely spaced stone columns reduced the magnitude of settlement of the embankment as well as the lateral displacement of the subsoil. The reduction in settlement and lateral displacement was 25% and 50% of that corresponding to the embankment with no ground improvement. Case 6 is

of an embankment supported by deep cement mixed (DCM) and stiffened deep mixed (SDCM) piles over soft Bangkok clay. The embankment load was transferred most efficiently to the SDCM pile than to the DCM pile, reflecting smaller settlement of the SDCM pile when compared to the DCM pile.

References

Journal Papers

Bergado, D.T., Lorenzo, G.A. and Long, P.V., Limit Equilibrium Method Back Analysis of Geotextile-Reinforced Embankments on Soft Bangkok Clay – A Case Study, *Geosynthetics International*, 9(3), 217-245, 2002.

Biot, M.A., General Theory of Three-Dimensional Consolidation, *Journal of Applied Physics*, 12, 155-164, 1941.

Broms, B. B. and Boman, P., Stabilization of Soil with Lime Columns, *Ground Engineering*, 12(4), 23-32, 1979.

Chai J.C. and Bergado D.T., Performance of Reinforced Embankment on Muar Clay Deposit, *Japanese Society of Soil Mechanics and Foundation Engineering*, 33(4), 1-17, 1993.

Chen, R.P., Xu, Z.Z., Ling, D.S. and Zhu, B., Field Tests on Pile-Supported Embankments over Soft Ground, *Journal of Geotechnical and Geoenvironmental Engineering*, 136(6), 777 – 785, June, 2010.

Davis, E.H. and Booker, J.R., The Effect of Increasing Strength with Depth on the Bearing Capacity of Clays, *Geotechnique*, 23(4), 551-563, 1973.

Giroud, J. P., Bonaparte, R., Beech, J. F. and Gross, B. A., Design of Soil Layer-Geosynthetic Systems Overlying Voids, *Geotextiles and Geomembranes*, Elsevier, 9(1), 11-50, 1990.

Hewlett, W. J., and Randolph, M. F., Analysis of Piled Embankments, *Ground Engrg.*, 21 (3), 12–18, 1988.

Indraratna, B., Balasubramaniam, A.S. and Ratnayake, P., Performance of Embankment Stabilized with Vertical Drains on Soft Clay, *Journal of Geotechnical Engineering*, 120(2), 257-273, Feb, 1994.

Kaniraj, S.R., Rotational Stability of Unreinforced and Reinforced Embankments on Soft Soils, *Journal of Geotextiles and Geomembranes*, 13(11), 707-726, 1994.

Leshchinsky, D., Short-term Stability of Reinforced Embankments over Clayey Foundation, *Soils and Foundations*, 27(3), 43-57, 1987.

Liu, H. L., Ng, C. W. W., and Fei, K., Performance of Geogrid-Reinforced and Pile-Supported Highway Embankment over Soft Clay: Case Study" *J. Geotechnical and Geoenvironmental Engrg.*, 133(12), 1483–1493, 2007.

Long, P.V., Bergado, D.T. and Balasubramaniam, A.S., Stability Analysis of Reinforced and Unreinforced Embankments on Soft Ground, *Geosynthetics International*, 3(5), 583-604, 1996.

Low, B.K., Wong, K.S. and Lim, C., Slip Circle Analysis of Reinforced Embankment on Soft Ground, *Journal of Geotextiles and Geomembranes*, 9(2), 165-181, 1990.

Rowe, R.K., Gnanendran, C.T., Landva, A.O. and Valsangkar, A.J., Construction and Performance of a Full-Scale Geotextile Reinforced Test Embankment, *Canadian Geotechnical Journal*, 32, 512-534, 1995.

Rowe, R.K. and Li, A.L., Geosynthetic-reinforced Embankments over Soft Foundations, *Geosynthetics International*, 12(1), 50-85, 2005.

Shukla, S.K. and Kumar, R., Overall Slope Stability of Prestressed Geosynthetic-Reinforced Embankments on Soft Ground, *Geosynthetics International*, 15(2), 165-171, 2008.

Tan, T. S., Inoue, T., and Lee, S. L., Hyperbolic Method for Consolidation Analysis, *Journal of Geotechnical Engineering*, 117(11), 1723–1737, 1991.

Tavenas, F., Jean, P., Leblond, P. and Leroueil, S., The Permeability of Natural Soft Clays. Part 2, Permeability Characteristics, *Canadian Geotechnical Journal*, 20, 645-660, 1983.

Books

Delmas, P., *Sols renforcés par géosynthétiques – premières études*, Thèse de l'université scientifique et médicale de Grenoble, Grenoble, France, 200p, 1979 (in French)

Milligan, V. and Busbridge, J. R., *Guidelines for the Use of Tensar in Reinforcement of Fills over Weak Foundations*. In: Golder Associates Report to the Tensar Corp., Mississauga, Ontario, Canada, 1983.

Jewell, R. A., *Soil Reinforcements with Geotextiles*, Thomas Telford, London, UK, Construction Industry Research and Information Association, CIRIA Special publication 123, 1996.

John, N. W. M., *Geotextiles*. Blackie & Son, London, UK, 1987.

Terzaghi, K., *Theoretical Soil Mechanics*, Wiley, New York, 510p, 1943.

Edited Volumes

Roscoe, K. H. and Burland, J.B., On the Generalized Stress-Strain Behaviour of Wet Clays, Engineering Plasticity, Cambridge, Cambridge Univ. Press, pp: 535-609, 1968.

Proceedings Papers

Aboshi, H., Ichimoto, E., Enoki, M., and Harada, K., The Compozer - A Method to Improve Characteristics of Soft Clays by Inclusion of Large Diameter Sand Columns, *Proceedings of International Conference on Soil Reinforcement*, 211-216, 1979.

Bonaparte, R. and Christopher, B. R., Design and Construction of Reinforced Embankments over Weak Foundations, *Symposium on Reinforced Layered Systems*, Transportation Research Record 1153, 26–39, TRB, Washington, DC, USA, 1987.

Bergado, D.T., Phienwej, N., Jamasawang, P., Ramana, G.V., Lin, S.S. and Abuel-Naga, H.M., Settlement Characteristics of Full Scale Test Embankment on Soft Bangkok Clay Improved with Thermo-PVD and Stiffened Deep Cement Mixing Piles, *Proceedings of 17th ICSMGE*, Alexandria, Egypt, 1969 – 1972, Oct, 2009.

Enoki, M., Yagi, N., Yatabe, R., and Ichimoto, E., Shearing Characteristics of Composite Ground and its Application to Stability Analysis, *Deep Foundation Improvements: Design, Construction, and Testing*, ASTM STP 1089, 19-31, 1991.

Houlsby, G. T. and Jewell, R. A., Analysis of Reinforced and Unreinforced Embankments on Soft Clays by Plasticity Theory, *Proc., International Conference on Numerical Methods in Geomechanics*, Innsbruck, Austria, Balkema, Rotterdam, The Netherlands, 2, 1443–1448, 1988.

Oh, E. Y. N., Balasubramaniam, A. S., Surarak, C. Bolton, M, Chai, G. W. K., Huang, M. and Braund, M., Behaviour of a Highway Embankment on Stone Column Improved Estuarine Clay, *Proc., 16th Southeast Asian Geotechnical Conference*, Malaysia, 1, 567-572, 2007.

Rowe, R.K. and Soderman, K.L., Reinforcement of Embankments on Soils whose Strength Increases with Depth, *Proceedings of Geosynthetics '87*, New Orleans, 266–277, 1987.

Rowe, R.K. and Mylleville, B.L.J., Consideration of Strain in the Design of Reinforced Embankments, *Proceedings of Geosynthetics '89*, San Diego, USA, 124–135, 1989.

Ting, W.H., Chan, S.F. and Kassim, K., Embankments with Geogrids and Vertical Drains, *Proc., International Symposium on Trial Embankments on Malaysian Marine Clays*, Kuala Lumpur, 2(21), 1-13, 1989.